

# PSO based Single and Two Interconnected Area Predictive Automatic Generation Control

MUHAMMAD S. YOUSUF      HUSSAIN N. AL-DUWAISH      ZAKARIYA M. AL-HAMOZ  
Department of Electrical Engineering  
King Fahd University of Petroleum & Minerals, Dhahran  
KINGDOM OF SAUDI ARABIA  
syousuf;hduwaish;zhamouz@kfupm.edu.sa

*Abstract:* This paper presents a Particle Swarm Optimization (PSO) based Model Predictive Control (MPC) scheme applied to Automatic Generation Control (AGC) systems. The proposed scheme formulates the MPC as an optimization problem and PSO is used to find its solution. Single area AGC model is taken incorporating Generation Rate Constraint (GRC) nonlinearities and constraints on the control input. Two interconnected area AGC system excluding nonlinearity is also studied. The simulation results draw several comparisons to preceding literature showing significant improvements and signifying the strengths of the proposed MPC scheme. Furthermore, performance of controller is also explored for varying power demands, different GRC values and parameter variations.

*Key-Words:* Model Predictive Control, Particle Swarm Optimization, Automatic Generation Control, Load Frequency Control, Nonlinear Predictive Control, Optimization Problem.

## 1 Introduction

Automatic Generation Control (AGC) has been one of the most important subjects for power systems engineers for decades as it is essential to maintain good quality and reliable electric power systems to the consumers. The main objectives of AGC for a power system includes Ensuring zero steady-state errors for frequency deviations, minimizing unscheduled tie line power flows between neighboring control areas, and minimizing the effect of load disturbances.

Today's large scale power systems are composed of interconnected subsystems or control areas in which the frequency of the generated power has to be kept constant. These subsystems are connected via tie-lines or HVDC links making distinct control areas. Each area has one or more generators and is responsible for its own loads as well as scheduled interchanges with neighboring areas. However, loading in power systems is never constant and changes in load result in changes in system frequency.

AGC has undergone extensive investigation because load frequency is such an important function of power system operation. A large portion of the study has considered linear AGC problems only. One of the earliest studies is by Cavin, which considers the AGC problem from an optimal stochastic control point of view [7]. The application of this technique resulted in improved transient response of the power and frequency deviations. However, this re-

quired the implementation of a fifth-order filter and was quite complex. A simpler technique based on PI optimal regulator is given in [6]. Other methods of classical control were also applied to LFC. However, with these methods, the dynamic performance was poor, especially with nonlinearities or parameter variations. Suboptimal control techniques have also been developed due to practical limitations of the optimal techniques [26], [9]. Early adaptive control techniques include those, as well as the PI adaptation technique given by Pan and Liaw [17]. It considers the plant parameter changes and instead of using an explicit parameter identification, the controller only used the available information of states and outputs fed back to it. Good results were obtained even with this reduced order plant model and the performance was somewhat insensitive to parameter variations and generation rate constant nonlinearity. Liaw has also presented a reduced order adaptive AGC technique for interconnected hydrothermal power system [16]. An adaptive decentralize AGC scheme for multi-area power systems is given by Zribi et al that guarantees very small fluctuations [32]. Another important technique applied to AGC has been the use of Variable Structure Control (VSC) [2], [4], [10]. Other schemes using GA have been also promoted in the literature, for example, GA and LMI based Robust LFC given in [21].

Although good linear control of multiarea load

frequency has been achieved by several researchers, these designs will not work properly in practice due to the real nonlinear nature of AGC systems. Therefore, consideration of nonlinearities in the models of AGC is very important. One of the main type of nonlinearities is the Generation Rate Constraint (GRC). This is the constraint on the power generation rate of the turbine and due to it the disturbance in one area affects the output frequency in other interconnected areas. The Governor Dead Band (GDB) is also another type of nonlinearity in the LFC systems [28].

For nonlinear system models of LFC, a Ricatti-based optimal technique is proposed by Wang [29]. The controller design is based on optimization of a Ricatti-equation. The results show large variations in frequency and power output and the system states take a long time to settle to steady state values. Using the proposed technique, these important problems will be tackled. Adaptive control provided a better control of the AGC problem, especially with the presence of nonlinearities and parameter variations [22], [1]. However, implementation limitations hamper its popularity. Velusami used decentralized biased dual mode controllers with for AGC nonlinearities [28]. The results showed good closed loop stability with high quality responses of the system for both steady and transient states while being less sensitive to parameter variations. Thus it appears that adaptive and decentralized control techniques for AGC give better results compared to conventional schemes.

For the past decade, researchers have focused on intelligent control schemes for nonlinear LFC as well. Birch gives an enhanced neural network LFC technique for the power system in England and Wales [5]. The NN approach has several advantages of conventional approaches, as the controller is able to perform well in case of parameter variations and time variance of the system, resulting in effective and robust control. However, the drawback is that the bulky neural network has to be trained offline and is not suitable for full closed loop control. It also has to be retrained in the case of system changes. ANN techniques for LFC systems are not uncommon, for example [23]. Shayeghi has also given an  $H_\infty$  based robust ANN LFC scheme [24]. Other ANN based techniques are given in good detail in the survey [25].

It is worthwhile to mention that none of the previous work on nonlinear AGC has handled the system constraints in the controller design process. Model predictive control (MPC) is a well-known control methodology that can easily incorporate and handle nonlinearities and constraints in the controller design. Although it has been extensively used in process control such as in [12] and as listed in [11], limited applications in power systems have been reported, for

example [15] and [27]. Recently, a new particle swarm based (PSO) based MPC controller is proposed in [31]. In this paper, the PSO-based MPC design method is applied multiarea nonlinear AGC system. The proposed approach will handle the nonlinearities and constraints in the AGC system in a structured way in the controller design process. This will give obvious advantages with regards to optimal control and constraints handling.

The paper is organized as follows: First the nonlinear AGC model is presented in Section 2, followed by an introduction to the proposed controller in Section 3. Section 4 gives simulation results and comparisons with previous work on AGC. Single area cases excluding and including GRC nonlinearities and two interconnected area cases excluding GRC nonlinearities are taken. Finally, conclusions are derived in Section 5.

## 2 Model of Automatic Generation Control System

The block diagram of an AGC system is given in Figure 1 as in [29] and the states of the system are:

$$\dot{X} = \left[ \Delta \dot{f}_i(t) \Delta \dot{P}_{g_i}(t) \Delta \dot{X}_{g_i}(t) \Delta \dot{P}_{c_i}(t) \Delta \dot{P}_{t_i}(t) \right]^T \quad (1)$$

The definitions of the symbols used in the model are as follows:

- $f_i$  : area frequency in  $i$ th area (Hz)
- $P_{g_i}$  : generator output for  $i$ th area (p.u. MW)
- $X_{g_i}$  : governor valve position for  $i$ th area (p.u. MW)
- $P_{c_i}$  : integral control value for  $i$ th area (p.u. MW)
- $P_{t_i}$  : tie line power output for  $i$ th area (p.u. MW)
- $P_{t_i}$  : load disturbance for  $i$ th area (p.u. MW)
- $T_{g_i}$  : governor time constant for  $i$ th area (s)
- $T_{p_i}$  : plant model time constant for  $i$ th area (s)
- $T_{t_i}$  : turbine time constant for  $i$ th area (s)
- $K_{g_i}$  : plant transfer function gain for  $i$ th area
- $R_i$  : speed regulation due to governor action for  $i$ th area (Hz p.u.  $MW^{-1}$ )
- $B_i$  : frequency bias constant for  $i$ th area (p.u. MW  $Hz^{-1}$ )

$a_{ij}$  : ratio between the base values of areas  $i$  and  $j$

The numerical values of these parameters are given in Section 4. The control objective of AGC is to keep the change in frequency,  $\Delta f_i(t) = x_1(t)$  as close to 0 as possible in the presence of load disturbance,  $d_i(t)$  by the manipulation of the input,  $u_i(t)$ . The detailed model of the system along with the values of state matrices can be found in [30].

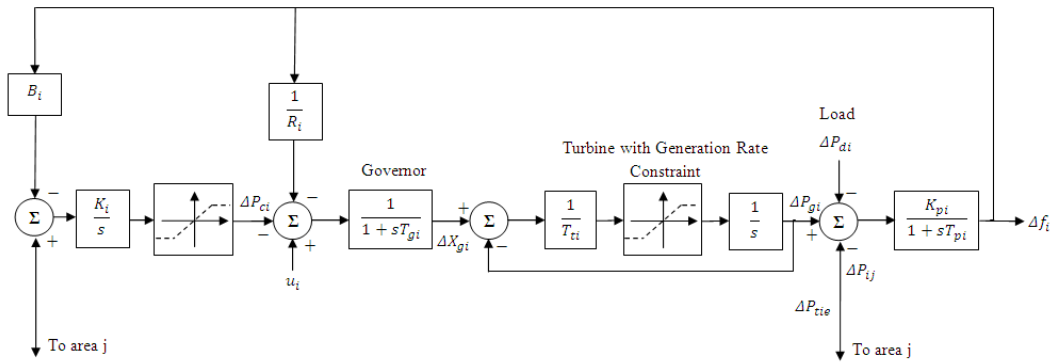


Figure 1: Block diagram of nth area AGC with GRC nonlinearities

### 3 Controller Structure

This section gives the basic structure of the proposed MPC-PSO controller.

#### 3.1 Model Predictive Control

It is recognized that linear control is not able to accurately control nonlinear processes and MPC is one of the most successful nonlinear control methodologies available today. Its main advantages are that it is able to systematically and directly handle process constraints during the controller design and can incorporate any cost function and process model. Its versatility is further enhanced by its ability to integrate with any optimization technique, for example PSO in this case. A good review of MPC can be found in [20].

Consider a discrete-time space with a sampling period  $T$ . The input and output of every system in this space will be denoted by  $\mathbf{u}[k] := \mathbf{u}(kT)$  and  $\mathbf{y}[k] := \mathbf{y}(kT)$  respectively, where  $k$  is an integer from  $-\infty$  to  $+\infty$ . Any nonlinear lumped system in this space can be described by the following sets of equations:

$$\mathbf{x}(k + 1) = \mathbf{h}(\mathbf{x}(k), \mathbf{u}(k), k) \quad (2)$$

$$\mathbf{y}(k + 1) = \mathbf{f}(\mathbf{x}(k), \mathbf{u}(k), k) \quad (3)$$

Where  $\mathbf{h}$  and  $\mathbf{f}$  are nonlinear functions of control input,  $u(k) \in u_{opt} \in \mathbb{R}^{n_u}$ , system states,  $x(k) \in \mathbb{R}^{n_x}$ , and process output,  $y(k) \in \mathbb{R}^{n_y}$  which are given at every time instant,  $k$ .

The future outputs of the system are determined for a finite period called the Prediction Horizon,  $H_p$ . These predicted outputs, denoted by  $\hat{\mathbf{y}} = [\hat{y}(k + 1), \hat{y}(k + 2), \dots, \hat{y}(k + H_p)]^T$  are dependent on the future control moves given by  $u = [u(k), u(k + 1), \dots, u(k + H_p - 1)]^T$  which are calculated by the optimization of a cost function,  $J$ . The objective is to keep the process as closed as possible to the reference

trajectory,  $w = [w(k + 1), w(k + 2), \dots, w(k + H_p)]^T$ . A generalized cost function is given as:

$$J = \sum_{i=1}^{H_p} e(k + i)^T Q e(k + i) + \sum_{i=1}^{H_c} \Delta u(k + i)^T R \Delta u(k + i) + \sum_{i=1}^{H_p} u(k + i)^T S u(k + i) \quad (4)$$

where  $H_c$  is the control horizon and  $e$  is the error between the desired output and the predicted output.

$$e = w(k) - \hat{y}(k) \quad (5)$$

$Q, R$  and  $S$  are the weighting matrices and penalize the error  $e$ , control effort  $u$ , and change in control effort  $\Delta u$  respectively. Their values are assigned according to the process model and constraints.

Figure 2 shows the behavior of predicted output and input over one such horizon.

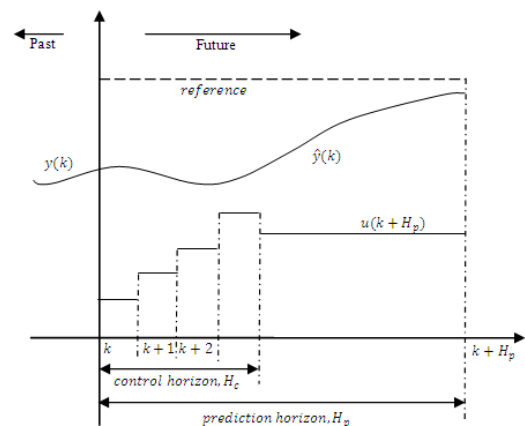


Figure 2: Predicted output and the corresponding optimal input over a horizon  $H_p$ .

When the controller output sequence,  $u(k)$  is obtained for controlling the process in the next  $H_p$  samples, only the first element of  $u(k)$  is used to control the process instead of the complete controller output sequence. At the next sample,  $k+1$ , the method is repeated using the latest measured information.

This is called the *receding horizon* principle and it is described more in [11]. Assuming that there are no disturbances or modeling errors, the predicted process output,  $\hat{y}(k+1)$  is exactly equal to the actual process output. The reason of using the receding horizon technique is that it allows for the compensation of future disturbances or modeling errors.

The structure of the control technique proposed here can be seen in Figure 3. The minimization of  $J$  is done by PSO which is described in Section 3.2.

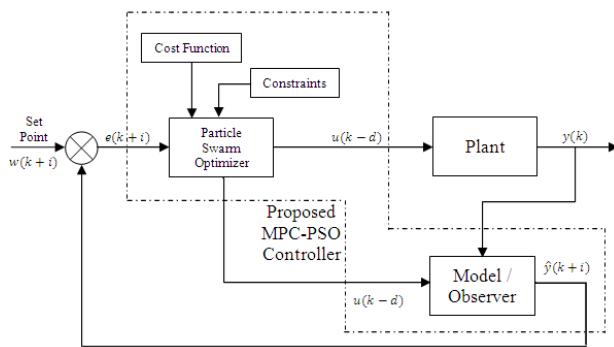


Figure 3: Structure of Proposed MPC-PSO Controller

The MPC algorithm can be summarily described to generally have the following three steps as in [20].

1. Explicit use of a model to predict the process output along a future time horizon (Prediction Horizon,  $H_p$ )
2. Calculation of a control sequence along a future time horizon (Control Horizon,  $H_c$ ), to optimize a performance index.
3. A *receding horizon* strategy, so that at each instant the horizon is moved towards the future which involves the application of the first control signal of the sequence calculated at each step.

### 3.2 Particle Swarm Optimization

PSO is one of the best known and widely used optimization methods. It was introduced by Eberhart & Kennedy [14] and incorporates three important properties of human or animal social behavior, which are evaluation, comparison, and imitation. Compared to other Evolutionary Algorithms (EAs), PSO is a more robust and faster algorithm that can solve nonlinear, non-differentiable, multi-modal problems which involve minimization of a objective function. This func-

tion will give the optimal control signals to the proposed controller.

Since PSO can generate a high-quality solution quickly with most stable convergence characteristics, it has been effective in solving problems to a wide variety of scientific fields as in and abundant literature is available on it. Kennedy gives details on how to avoid bad practices while using the PSO algorithm for effective use [13]. The details of PSO can be studied in the various sources cited in this paragraph.

### 3.3 Proposed MPC-PSO Method Summary

#### 3.3.1 Controller Objective

Given a linear or nonlinear plant, the controller objective is to construct the PSO based predictive controller such that it searches for the optimal control signals and minimizes the error in the minimum time using minimum effort in the presence of disturbances and constraints.

#### 3.3.2 Algorithm Implementation

The algorithm is implemented as follows:

1. Initialize particles at the start by assigning them random values.
2. Generate set of inputs for the process and apply to the model.
3. Evaluate cost function based on the model's output.
4. Evaluate fitness function, which is the inverse of cost function:  $fitness = 1/|J|$
5. Based on fitness, find optimal input sequence consisting of physical control moves or signals using PSO.
6. Update particles with these values and apply them to the model again, repeating a certain number of times.
7. Apply the first optimal control signal to the system and repeat these steps for next samples.

The number of particles represent the prediction horizon,  $H_p$  and it is taken as 5. The swarm size is 50 and the number of iterations of the swarm per sample is 500, which ensures that the swarm converges to an optimal solution. The PSO parameters,  $c_1$  and  $c_2$  are both set at 2.04 after several trials. A time varying weighting factor is used that varies from 0.4 to 0.9 as the swarm progresses in the solution space.

## 4 MPC-PSO for Automatic Generation Control

In this section, the simulation results for the application of the proposed technique on single and two area

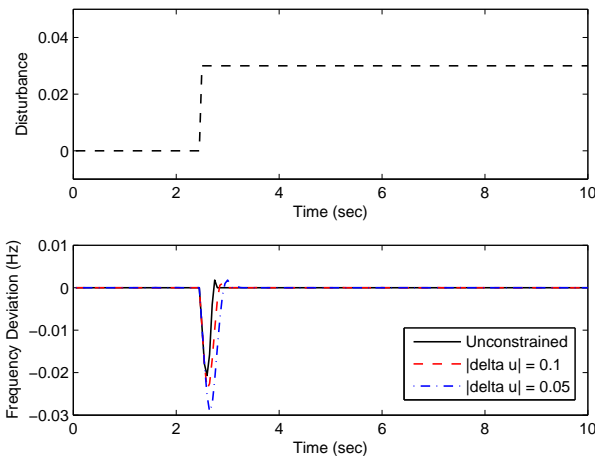


Figure 4: Case I A - Disturbance and Frequency Deviation for Designs 1-3

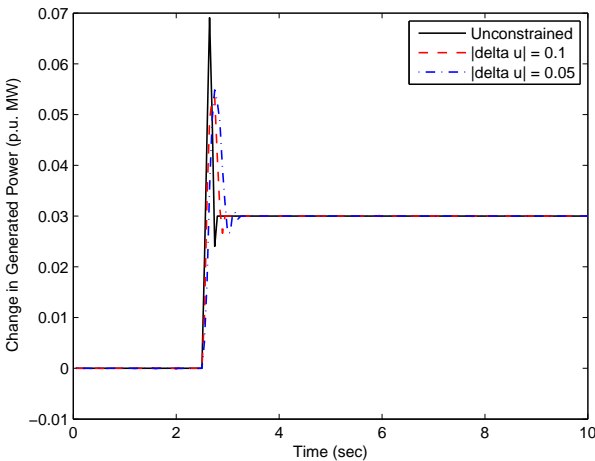


Figure 5: Change in Generated Power for Designs 1-3

AGC systems are given.

### 4.1 Part I - Performance of Single Area AGC Excluding GRC Nonlinearities

First, the single area AGC system excluding the GRC nonlinearity is studied. The system parameters are computed using the following values:

$$T_s = 20s, K_p = 120 \text{ Hz p.u. MW}^{-1}, T_t = 0.3s, K = 0.6 \text{ p.u. MW}^{-1} \text{ rad}^{-1}, T_g = 0.08s, R = 2.4 \text{ Hz p.u. MW}^{-1}$$

The system is given a step change of 0.3 p.u. Naturally, this change in load will demand the system to adjust its power output by the same amount. This will change the load frequency which needs to be minimized and brought to zero as soon as possible while obeying the constraints of the system and control effort. The cost function for the single area case is taken

as:

$$J = \sum_{i=1}^{H_p} \Delta f_1(t)^2 + \Delta P_{g1}^2$$

#### 4.1.1 Case A - System Under Constant Disturbance and Different Constraints on $\Delta u$

The behavior of the system is studied under three conditions. In all these, the limits of the control signal are imposed to be,

$$-0.2 \leq u \leq 0.2$$

These conditions are designed on the basis of constraints on the control effort as:

- Design 1 - No constraint on change in the control effort between samples, i.e.  $\Delta u$  is unconstrained.
- Design 2 -  $\Delta u \leq 0.1$ . This means that the control effort cannot change by more than 50% between samples.
- Design 3 -  $\Delta u \leq 0.05$ . This means that the control effort cannot change by more than 25% between samples.

Figure 4 shows the disturbance of 0.3 p.u. applied to the system and the corresponding frequency deviation observed. It is observed that the disturbance causes the least frequency deviation for the case when the control effort is unconstrained between samples. The reason is obvious. The frequency deviates to a maximum value of -0.02 p.u. For the case of constrained  $\Delta u$ , the frequency deviation is relatively large, up to a value of 0.03 p.u. However, it is also observed that for the case of unconstrained  $\Delta u$ , the change in generated power is larger than the case with constrained  $\Delta u$  as shown in Figure 5. This means that to change the output power with respect to the load disturbance, there momentarily is an overshoot going up to 0.07 p.u. which for the case of constrained  $\Delta u$  is only up to 0.05. After this value, the generated power steadily drops to the required 0.03 p.u. value. Same is true for the small undershoot. Understandably, it takes more time to achieve the results in the case of constrained  $\Delta u$ .

#### 4.1.2 Case B - System Under Varying Disturbance

To study the robustness of the proposed controller for the case of varying load disturbances, a load disturbance seen in Figure 6 is applied. The load is simulated to vary from a disturbance of 0 p.u. to 0.03 p.u.,

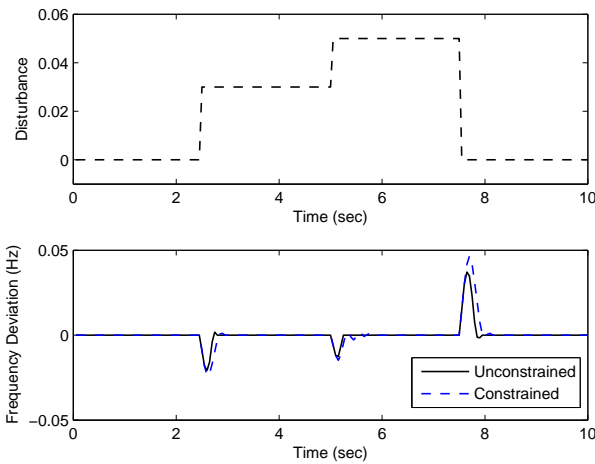


Figure 6: Case I B - Varying Disturbance and Frequency Deviation

going up to 0.05 p.u. and then becoming 0 p.u. again. This effect of the varying load is on the load frequency is also seen in this figure. It is seen that the load frequency varies most when the disturbance varies most. When the disturbance varies from 0.05 p.u. to 0, the load frequency varies maximum for the case of controller with constrained  $\Delta u$ , going up to a maximum frequency disturbance of 0.05 p.u. and 0.045 p.u. for the case of unconstrained  $\Delta u$ . The corresponding behavior of the change in generated power is seen in the Figure 7. It is seen that the change in generated power follows the load disturbance meaning that the system can supply the load its power demand. The power generated changes most when the disturbance is largest. Also, the trade off seen in the previous results is also apparent here, that the change in generated power is more for the case of unconstrained  $\Delta u$ , however the frequency deviation is large and vice versa for the case of constrained  $\Delta u$ . It is also seen that the change in generated power takes a few more instances to arrive at the steady state for the case of constrained  $\Delta u$ . This behavior is in line with the observations of the previous case as well.

### 4.2 Part II - Performance of Single Area AGC Including GRC Nonlinearities

Now, the GRC nonlinearities are included. They appear in the system in the form of saturation of states and are illustrated in Figure 1.

The constraint on the control signal is:

$$-0.5 \leq u \leq 0.5$$

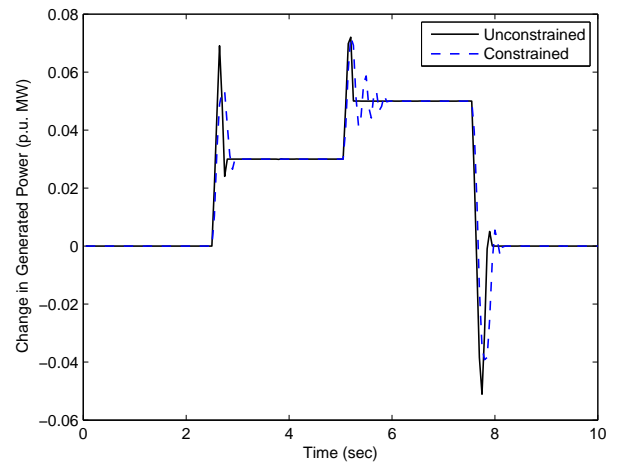


Figure 7: Varying Disturbance and Change in Generated Power

### 4.3 Case A - System with GRC=0.0017 p.u. MW sec<sup>-1</sup>

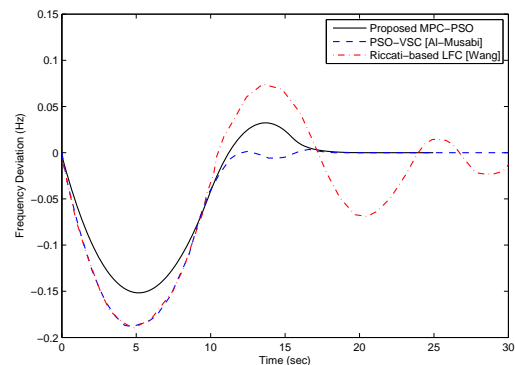


Figure 8: Case II A - Frequency Deviation for GRC = 0.0017

The system is tested for a GRC value of 0.1 p.u.  $MW \min^{-1} = 0.0017 \text{ p.u. } MW \text{ sec}^{-1}$ , as done in previous work by Al-Musabi [3] and Wang [29]. This means that the generated power output of the system cannot vary by more than 0.0017 p.u. MW in 1 second. A disturbance of 0.01 p.u. is present in the system. The proposed controller is applied to the system with this nonlinearity.

The results of this test can be seen in Figures 8 and 9. It is seen that the proposed technique performs much better than that Riccati-based optimal load frequency controller proposed by [29]. Comparing with the PSO-VSC technique given by [3], the settling time of the system is same, however there is lesser undershoot in frequency deviation. It can be seen in Figure

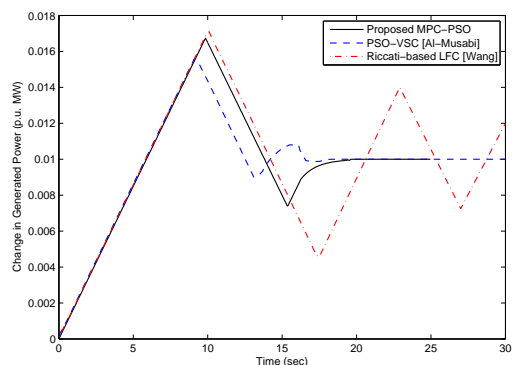


Figure 9: Generated Power Output for GRC = 0.0017

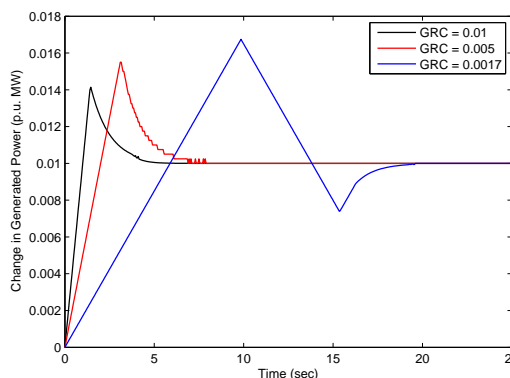


Figure 11: Generated Power Output for Varying GRC

8, that the maximum frequency deviation of the system using the proposed technique is lesser than the previous work for this value of GRC.

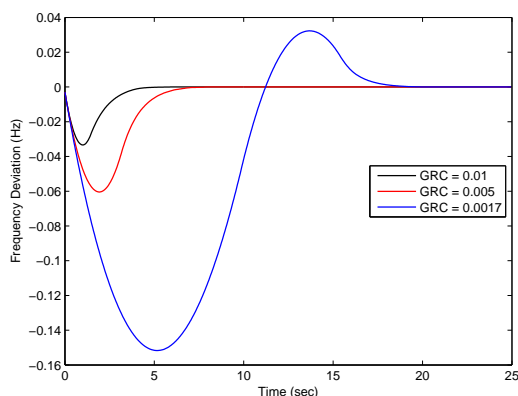


Figure 10: Case II B - Frequency Deviation for Varying GRC

#### 4.4 Case B - System Comparison with Different GRC Values

A range of benchmark GRC values are applied and the system is tested for three cases. The values of GRC selected to be are 0.0017, 0.005 and 0.01. These GRC values are practical values and are dependent on the model and specifications of the power generation unit (turbine). All other parameters and control variables are same.

The results are seen in Figures 10 and 11. It is clear that the frequency deviation and the change in generated power is most for the case when the GRC is the smallest. The frequency deviates by as much as 0.152 Hz in this case and becomes 0 only after 19 seconds. The maximum value of the change in generated power is different in each case. It is 0.014, 0.016

and 0.017 for the cases when GRC is 0.01, 0.005 and 0.0017 respectively. When the GRC is smallest at 0.0017 p.u., it takes longest, i.e. 20s for the system to provide the steady demand power of 0.01 p.u. MW. For the cases of GRC 0.01 and 0.005, it took 5 and 8 seconds respectively.

From the behavior of the control inputs, it was observed that they vary till the time it takes for the system to reach the required steady states, after which they take their steady states. It was also observed that the cost is also the most for the case of smallest GRC and least for the case with the largest.

#### 4.5 Case C - System with GRC=0.01 p.u. MW sec<sup>-1</sup> and Varying Disturbance

Another challenging test for the AGC system is through varying the load disturbance. A varying load disturbance, as seen in Figure 13 is applied to the single area system with GRC = 0.01 p.u. MW sec<sup>-1</sup>. The load disturbance is 0.01 p.u. at the start and then changes to 0.02 and 0.03 p.u., and finally becomes 0.015 p.u. The dynamics of the frequency deviation and change in generated power are seen in Figures 12 and 13 respectively. It is seen that the frequency deviates by 0.033 p.u. every time an incremental disturbance of 0.01 p.u. is given at the load. The frequency deviation is maximum at 0.07 p.u. when the load disturbance changes by 0.015 p.u. at 60s. The generated power from the system fulfills the load demand in all cases as seen from Figure 13.

#### 4.6 Case D - System with GRC=0.01 p.u. MW sec<sup>-1</sup> and Parameter Variations

A challenging case involving two parts is considered here:

- 25% parameter variations in the system due to severe disturbances or modeling errors

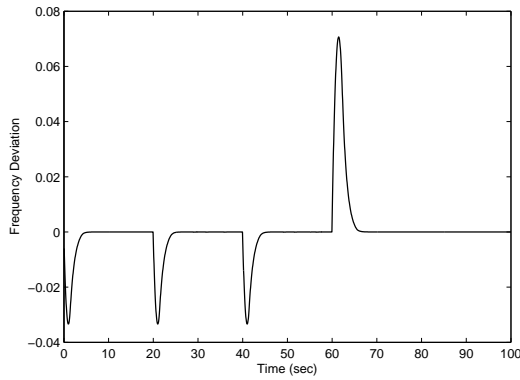


Figure 12: Case II C - Frequency Deviation for Varying Disturbance

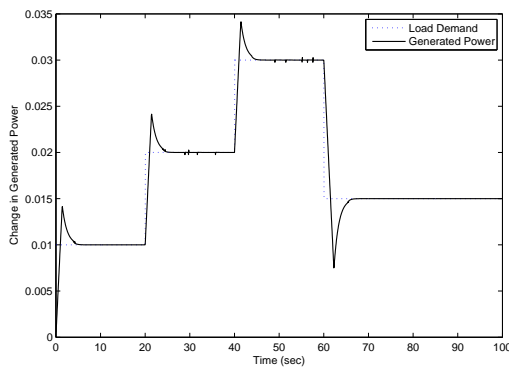


Figure 13: Applied Varying Disturbance and Generated Power Output

- GRC nonlinearity of 0.01 p.u.  $MW sec^{-1}$  applied on two states,  $x_2$  and  $x_4$

The corresponding values of A, B & F are:

$$A = \begin{bmatrix} -0.0665 & 8 & 0 & 0 \\ 0 & -3.663 & 3.663 & 0 \\ -6.86 & 0 & -13.736 & -13.736 \\ 0.6 & 0 & 0 & 0 \end{bmatrix}$$

$$B = \begin{bmatrix} 0 & 0 & 13.736 & 0 \end{bmatrix}^T$$

$$F = \begin{bmatrix} -8 & 0 & 0 & 0 \end{bmatrix}^T$$

The results of this comparison are given in Figures 17 to 20. It is seen that the frequency deviates by 33% more for the case when system parameters are varied by 25%. However, in this case it takes a little less time to reach the required value. The change in generated power almost remains the same for both cases. There is slight difference in the behavior which

is clear from Figure 18. The change in generated power is observed to be 25% more for the case with parameter variation. The results indicate that the proposed controller is quite indifferent to the variation in system parameters.

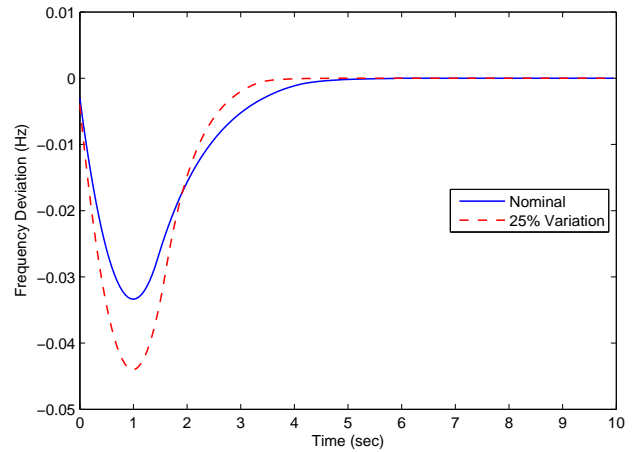


Figure 14: Case II D - Frequency Deviation for GRC with Parameter Variation

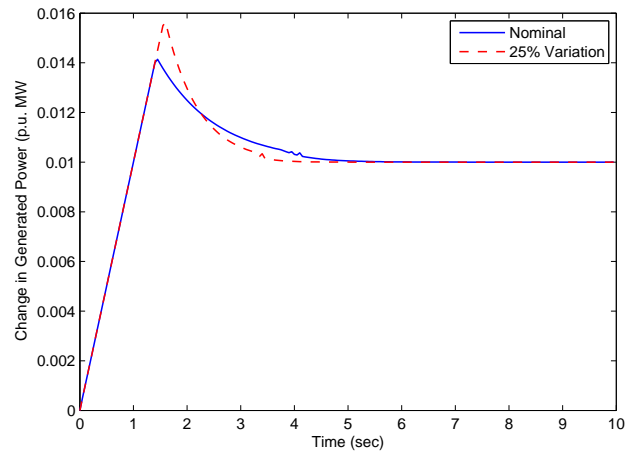


Figure 15: Generated Power Output for GRC with Parameter Variation

### 4.7 Part III - Performance of Two Inter-connected Areas AGC System Excluding GRC Nonlinearities

In this section, the AGC problem is extended to two interconnected areas. The areas are connected as seen in Figure 16.

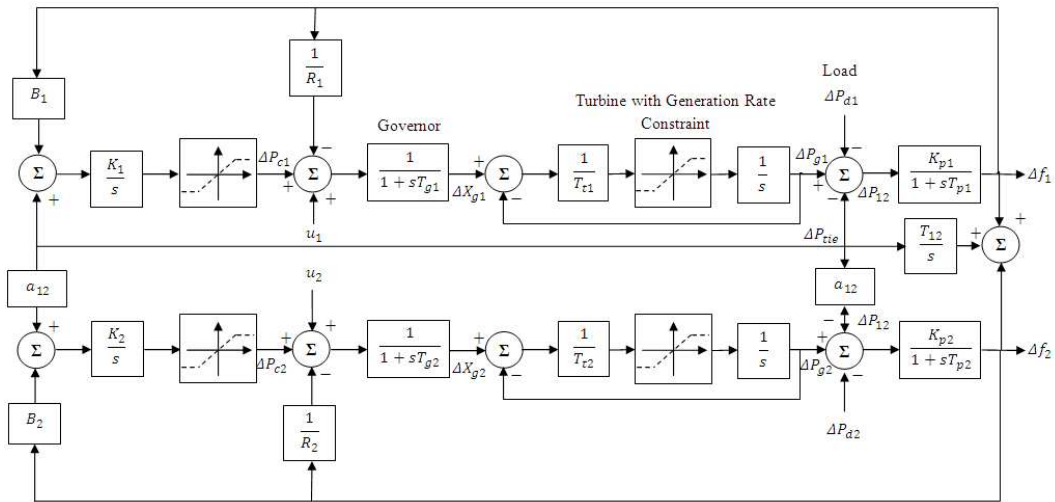


Figure 16: Block diagram of two-area AGC

The model in Figure 16 can be expressed by the following set of equations.

$$\dot{X}_i(t) = A_i x_i(t) + B_i u_i(t) +$$

$$\sum_{j=1, j \neq i}^n E_{ij} x_j(t) + F_i d_i(t) \quad (6)$$

$$y_i(t) = C_i(t) x_i(t) \quad (7)$$

$$\dot{X}^T = [\Delta \dot{f}_1(t) \Delta \dot{P}_{g1}(t) \Delta \dot{X}_{g1}(t) \Delta \dot{P}_{c1}(t) \Delta \dot{P}_{tie}(t)$$

$$\Delta \dot{f}_2(t) \Delta \dot{P}_{g2}(t) \Delta \dot{X}_{g2}(t) \Delta \dot{P}_{c2}(t)] \quad (8)$$

$$A = \begin{bmatrix} -\frac{1}{T_{p1}} & \frac{K_{p1}}{T_{p1}} & 0 & 0 & -\frac{K_{p1}}{T_{p1}} \\ 0 & -\frac{1}{T_{t1}} & \frac{1}{T_{t1}} & 0 & 0 \\ -\frac{1}{R_1 T_{g1}} & 0 & \frac{-1}{T_{g1}} & \frac{1}{T_{g1}} & 0 \\ -K_1 B_1 & 0 & 0 & 0 & -K_1 \\ T_{12} & 0 & 0 & 0 & 0 \\ 0 & 0 & 0 & 0 & \frac{K_{p2}}{T_{p2}} \\ 0 & 0 & 0 & 0 & 0 \\ 0 & 0 & 0 & 0 & 0 \\ 0 & 0 & 0 & 0 & K_2 \\ 0 & 0 & 0 & 0 & 0 \\ 0 & 0 & 0 & 0 & 0 \\ 0 & 0 & 0 & 0 & 0 \\ -T_{12} & 0 & 0 & 0 & 0 \\ -\frac{1}{T_{p2}} & \frac{K_{p2}}{T_{p2}} & 0 & 0 & 0 \\ 0 & -\frac{1}{T_{t2}} & \frac{1}{T_{t2}} & 0 & 0 \\ -\frac{1}{R_2 T_{g2}} & 0 & \frac{-1}{T_{g2}} & \frac{1}{T_{g2}} & 0 \\ -K_2 B_2 & 0 & 0 & 0 & 0 \end{bmatrix} \quad (9)$$

$$B^T = \begin{bmatrix} 0 & 0 & \frac{1}{T_{g1}} & 0 & 0 \\ 0 & 0 & 0 & 0 & 0 \\ 0 & 0 & \frac{1}{T_{g2}} & 0 & 0 \end{bmatrix} \quad (10)$$

$$C = \begin{bmatrix} 1 & 0 & 0 & 0 & 0 & 0 & 0 & 0 & 0 \\ 0 & 0 & 0 & 0 & 0 & 1 & 0 & 0 & 0 \end{bmatrix} \quad (11)$$

The system is stable and the objective is to minimize the system frequency deviation  $\Delta f_1(t)$  and  $\Delta f_2(t)$  in Areas 1 and 2 respectively under load disturbances in both areas.

#### 4.7.1 Case A - System with Matching Parameters and 3% Disturbance

The parameters of the system are given below [30]:  
 $T_{p1} = T_{p2} = 20s$ ,  $K_{p1} = K_{p2} = 120 \text{ Hz p.u. MW}^{-1}$ ,  $T_{t1} = T_{t2} = 0.3s$ ,  $K_1 = K_2 = 1 \text{ p.u. MW}^{-1} \text{ rad}^{-1}$ ,  $T_{g1} = T_{g2} = 0.08s$ ,  $R_1 = R_2 = 2.4 \text{ Hz p.u. MW}^{-1}$  and  $B_1 = B_2 = 0.425 \text{ p.u. MW Hz}^{-1}$

Since the parameters in this model are identical, and the change in the tie-line power,  $\Delta P_{tie}$  is caused by the difference in the area frequencies,  $\Delta f_1(t) - \Delta f_2(t)$ , the performance of the system has been tested by applying the disturbance in Area 1 only.

A step disturbance of 0.03 p.u. is applied constantly on the system in Area 1. The cost function in this case is taken to be as follows:

$$J = \sum_{i=1}^{H_p} \Delta f_1(t)^2 + \Delta f_2(t)^2 + \Delta P_{tie}^2 + \Delta P_{g1}^2 + \Delta P_{g2}^2$$

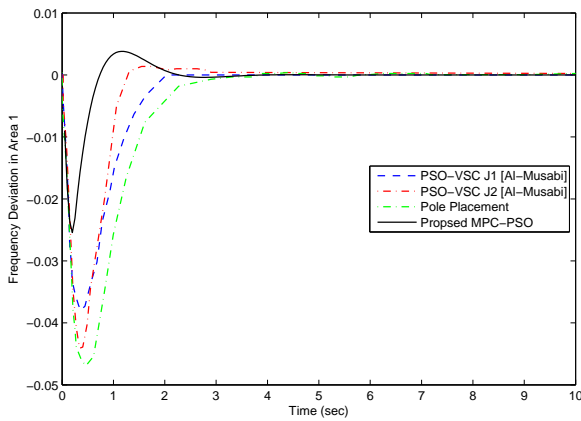


Figure 17: Case III A - Frequency Deviation in Area 1

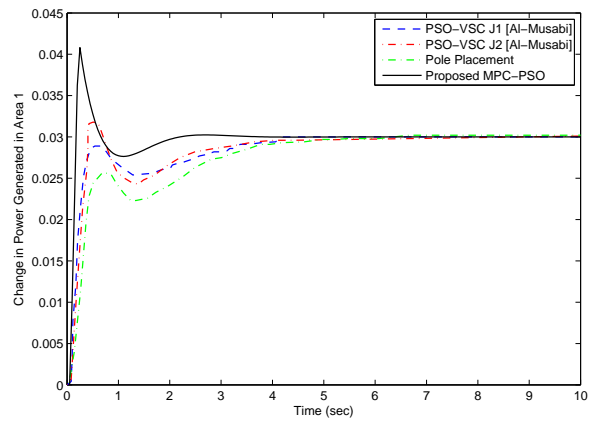


Figure 19: Case III A - Change in Generated Power in Area 1

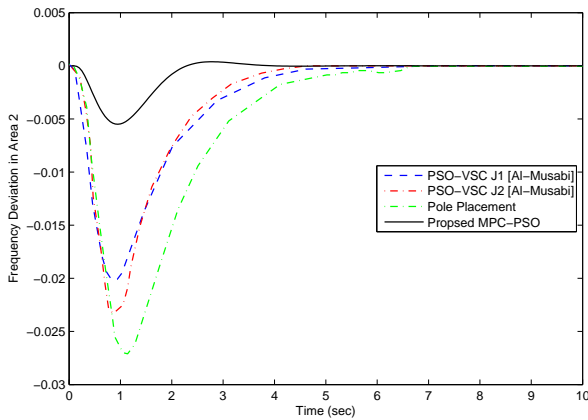


Figure 18: Frequency Deviation in Area 2

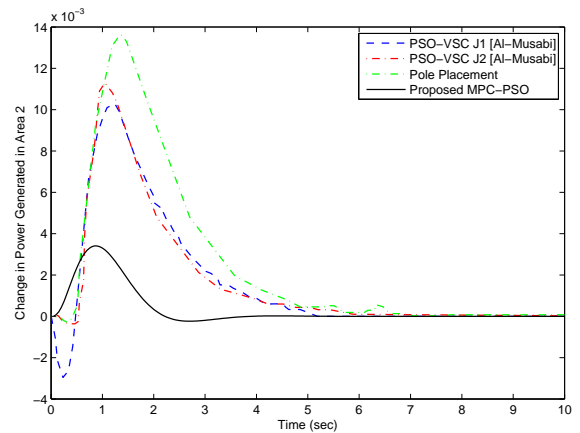


Figure 20: Change in Generated Power in Area 2

Such a cost function ensures that the system is internally stable. The terms of the cost function are scaled equally. The control signals in this case are constrained stringently to be  $-0.1 \leq u \leq 0.1$ . Since the control signal is already so much constrained within its maximum limit, there is no limit on the change of control,  $\Delta u$ .

The dynamics of the system in this case are given in Figures 17 to 20 and the results are compared with previous work [4] as well as LFC using the pole placement technique. The behavior of the frequency deviation in both areas is seen as well as the change in generated power in both areas. In comparison with the PSO-VSC technique two cost functions are compared.  $J_1$  is the same cost function used here, while  $J_2$  proposed in [4] is a slightly different cost function as it incorporates the control inputs into it as well. The results show the the proposed technique performs much better in all aspects as compared with the previous work. It is seen in Figure 17 that the frequency

deviation in Area 1 is less than what it was in the previous work as well as using the pole placement technique. Also, the frequency deviation becomes zero quicker using the proposed technique, than using previous techniques. From Figure 18, it is seen that for the Area 2, the deviation is at least 75% lesser compared to previous work.

It is seen in Figure 19 that the system is supplying the required 0.03 p.u. load from Area 1. The required load is supplied much quicker than in the compared techniques. But the trade-off for it is that the maximum change in generated power using the proposed technique is 0.01 p.u. more than previous work. There is minor deviation of generated power in Area 2, and it is must less compared to the deviation that is observed using other techniques. After that, the change in generated power in Area 2 becomes zero. Figure 21 shows the change in the tie-line power flow. Due to the frequency deviation in both areas, power begins to

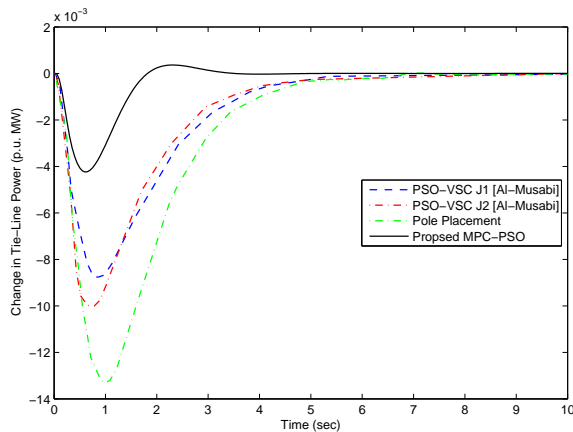


Figure 21: Case III A - Power Flow in Tie-Line

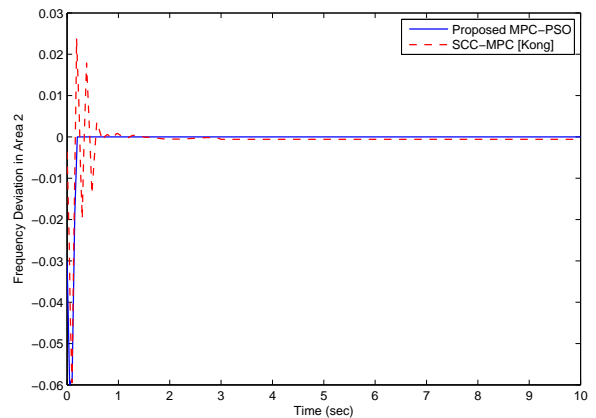


Figure 23: Frequency Deviation in Area 2

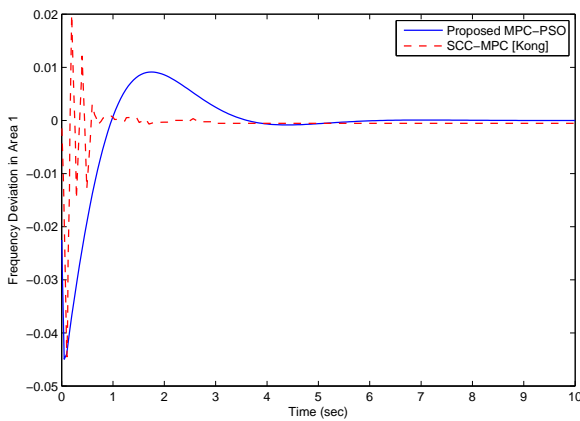


Figure 22: Case III B - Frequency Deviation in Area 1

flow in the tie-line and as soon as the frequency deviations reach 0, the power flow in the tie-line also stops. Compared to previous work and the pole placement technique, the power flow in the tie-line is much less using the proposed technique. The maximum flow in the tie-line in this case is -0.004 p.u., while for the pole placement technique, it is about 0.013 p.u.

#### 4.7.2 Case B - System with Mismatching Parameters and 10% Disturbance

Now a more challenging case of two-area AGC is studied. In this case the parameters of the two areas differ in the following respects:

$$T_{p1} = 25s, T_{p2} = 20s, K_{p1} = 112.5 \text{ Hz p.u. MW}^{-1}, K_{p2} = 120 \text{ Hz p.u. MW}^{-1}.$$

The rest of the system parameters are same as in Case A. This two-area system is subjected to a huge disturbance of 0.1 p.u. in both areas. This case is taken from the work done by Kong [15], in which

State Contractive Constraint (SCC)-based MPC is applied to the LFC problem. The comparison of the proposed technique with SCC-MPC is given in Figures 22 to 25. It is seen that the proposed MPC-PSO technique gives a much smoother control of the system. From Figure 22 it is clear that although the SCC-MPC is able to bring the Area 1 frequency deviation to zero 1 second earlier than MPC-PSO, there are a lot of oscillations and there is also a steady state error using the SCC-MPC technique. The proposed technique enables the Area 1 frequency deviation to become zero more smoothly and accurately. The frequency deviation in Area 2 is seen in Figure 23. It is seen that proposed technique fares enormously better than SCC-MPC. The change in generated power from the areas is seen in Figures 24 and 25. It is seen that the proposed techniques enables the system to cope with the power demand more smoothly, with lesser overshoot and shorter duration without any steady state errors. Since [15] does not give any details on the control constraints, they are taken to be  $-0.5 \leq u \leq 0.5$ .

It is seen that after 5s, once all the required states of the system are at equilibrium, the power in the tie-line also becomes zero.

## 5 Conclusion

The following conclusions can be drawn from this paper:

1. A new and efficient PSO based MPC scheme is designed. Unlike other control schemes, it can incorporate constraints in the controller design stage, thus giving it the attractive advantages of speed, accuracy and optimal control. Furthermore, application of MPC to the field of power systems extends its applications portfolio.
2. The dynamical behavior of the single nonlinear

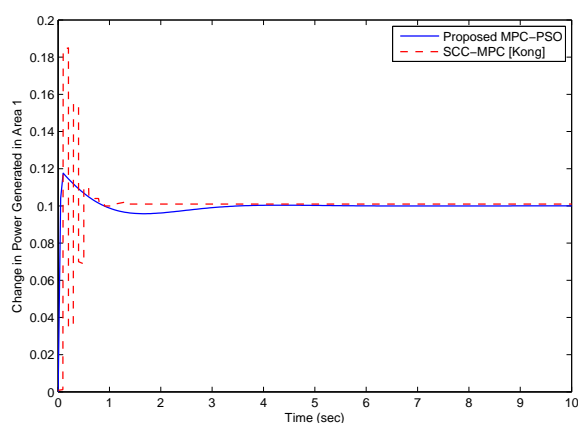


Figure 24: Case III B - Change in Generated Power in Area 1

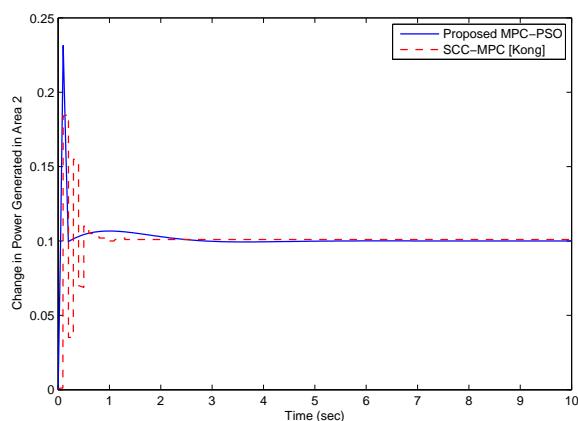


Figure 25: Change in Generated Power in Area 2

AGC system is explored with constraints on the control input. Comparison with the previous work using different control schemes shows that MPC-PSO gives reduced settling time and lower overshoots compared to Ricatti-VSC and PSO-VSC.

3. The proposed controller performs well for a range of practical GRC values.

4. The performance of the controller is satisfactory under rapid load variations and parameter variations.

5. The comparison of dynamical behavior of two interconnect area AGC system with similar cases from the preceding literature shows significant improvements and demonstrates the fact that the proposed technique is more suitable for such applications.

**Acknowledgements:** The authors would like to thank King Fahd University of Petroleum and Minerals, Dhahran, Saudi Arabia for providing support and resources to undertake this research.

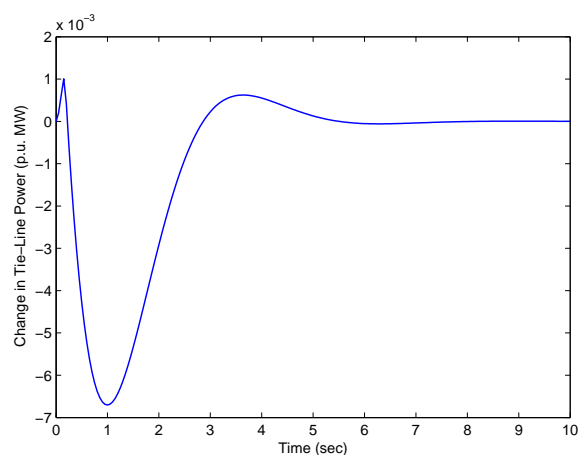


Figure 26: Case III B - Power Flow in Tie-Line

### References:

- [1] M. Aghdaie and M. Rashidi, *Robust and Adaptive Load Frequency Control of Multiarea Power Systems with system parametric uncertainties via TDMLP*, WSEAS Transactions on Systems, Vol. 3, No. 2, 2004, pp. 1001–1008.
- [2] Z. Al-Hamouz and H. Al-Duwaish, *A New Load Frequency Variable Structure Controller Using Genetic Algorithms*, Electric Power Systems Research, Vol. 55, 2000, pp. 1–6.
- [3] N. Al-Musabi, Z. Al-Hamouz, H. Al-Duwaish, and S. Al-Baiyat, *Variable Structure Load Frequency Controller using the Particle Swarm Optimization Technique*, Proceedings of the 10th IEEE International Conference on Electronics, Circuits and Systems, 2004, pp. 380–383.
- [4] Z. Al-Hamouz, N. Al-Musabi, H. Al-Duwaish, and S. Al-Baiyat, *Variable Structure Load Frequency Controller using the Particle Swarm Optimization Technique*, Electric Power Components and Systems, Vol. 33, 2005, pp. 1253–1267.
- [5] A. P. Birch, A. T. Sapeluk and C. S. Özveren, *An Enhanced Neural Network Load Frequency Control Technique*, IEE International Conference on Control, Vol. 389, 1994, pp. 409–415.
- [6] M. Calovic, *Linear Regulator Design for Load and Frequency Control*, IEEE Winter Power Meeting, 1971.
- [7] R. Cavin, M. Budge and P. Rasmussen, *An Optimal Linear Systems Approach to Load Frequency Control*, IEEE Winter Power Meeting, 1970.
- [8] S. S. Choi, H. K. Sim and K. S. Tan, *Load Frequency Control via Constant Limited-state Feed-*

- back, *Electric Power Systems Research*, Vol. 4, No. 4, 1981, pp. 265–269.
- [9] W. C. Chan and Y. Y. Hsu, *Automatic Generation Control of Interconnected Power System using Variable Structure Controllers*, Proceedings of the IEE Part C, Vol. 128, No. 5, 1981, pp. 269–279.
- [10] S. P. Ghosh, *Optimizations of PID Gains by Particle Swarm Optimizations in Fuzzy based Automatic Generation Control*, *Electric Power Systems Research*, Vol. 72, No. 3, 2004, pp. 203–212.
- [11] J. M. Maciejowski, *Predictive Control with Constraints*, Pearson Education Limited, 2002.
- [12] A. H. Mazinan and N. Sadati, *Multiple Modeling and Fuzzy Predictive Control of a Tubular Heat Exchanger System*, *WSEAS Transactions on Systems and Control*, Vol. 3, No. 4, 2008, pp. 249–258.
- [13] J. Kennedy, *Some Issues and Practices for the Particle Swarms*, Proceedings of the IEEE Swarm Intelligence Symposium, 2007, pp. 162–169.
- [14] J. Kennedy and R. Eberhart, *Particle Swarm Optimization*, Proceedings of the IEEE International Conference on Neural Networks, Vol. 4, Perth, Australia, 1995, pp. 1942–1948.
- [15] L. Kong and L. Xiao, *A New Model Predictive Control Scheme based Load Frequency Control*, IEEE International Conference on Control and Automation, 2007, pp. 2514–2518.
- [16] C. M. Liaw, *Design of a Reduced-order Adaptive LFC for an Interconnected Hydrothermal Power System*, *International Journal of Control*, Vol. 60, No. 6, pp. 1051–1063.
- [17] C. T. Pan and C. M. Liaw, *An Adaptive Controller for Power System and Load Frequency Control*, *IEEE Transactions on Power Systems*, Vol. 4, No. 1, 1980, pp. 122–128.
- [18] K. E. Parsopoulos and M. N. Vrahatis, *On the Computation of all Global Minimizers through Particle Swarm Optimization*, *IEEE Transactions on Evolutionary Computing*, Vol. 8, 2004, pp. 211–224.
- [19] D. M. Prett, C. E. Garcia, and M. Morari, *Model Predictive Control: Theory and Practice - a Survey*, *Automatica*, Vol. 25, No. 3, 1989, pp. 335–348.
- [20] S. J. Qin and T. A. Badgwell, *An Overview of Industrial Model Predictive Control Technology*, 1997, Available online at: <http://citeseerx.ist.psu.edu/viewdoc/summary?doi=10.1.1.52.8909>
- [21] D. Rerkpreedapong, A. Hasanovic and A. Feliachi, *Robust Load Frequency Control Using Genetic Algorithms and Linear Matrix Inequalities*, *IEEE Transactions on Power Systems*, Vol. 18, No. 2, 2003, pp. 855–861.
- [22] C. W. Ross, *Error Adaptive Control Computer for Interconnected Power System*, *IEEE Transactions on Power Apparatus and Systems*, Vol. 85, No. 7, 1966, pp. 742–749.
- [23] H. A. Shayanfar, *Decentralized Load Frequency Control of a Deregulated Electric Power System Using ANN Technique*, *WSEAS Transactions on Circuits and Systems*, Vol. 4, No. 1, 2005, pp. 32–37.
- [24] H. Shayeghi, H. A. Shayanfar, and A. Jalili, *Load Frequency Control Strategies: A State-of-the-Art Survey for the Researcher*, *Journal of Energy Conversion and Management*, Vol. 50, No. 1, 2009, pp. 344–353.
- [25] H. Shayeghi and H. A. Shayanfar, *Application of ANN Technique for Interconnected Power System Load Frequency Control*, *International Journal of Energy*, Vol. 16, No. 3, 2003, pp. 246–254.
- [26] G. Shirai, *Load Frequency Control Using Lyapunov's Second Method: Bang-Bang Control of Speed Changer Position*, Proceedings of the IEEE, Vol. 67, No. 10, 1979, pp. 1458–1459.
- [27] I. I. Siller-Alcalá, M. Abderrahim, J. Jaimes-Ponce, and R. Alcántara-Ramírez, *Speed-sensorless Nonlinear Predictive Control of a Squirrel Cage Motor*, *WSEAS Transactions on Systems and Control*, Vol. 3, No. 2, 2008, pp. 99–104.
- [28] S. Velusami and I. A. Chidambaram, *Decentralized biased Dual Mode Controllers for Load Frequency Control of Interconnected Power Systems considering GDB and GRC Nonlinearities*, *Journal of Energy Conversion and Management*, Vol. 48, No. 1, 2007, pp. 1691–1702.
- [29] Y. Wang, R. Zhou, and C. Wen, *Robust Load Frequency Controller Design for Power Systems*, *IEE Proceedings-C*, Vol. 140, No. 1, 1993, pp. 11–16.
- [30] T. C. Yang, H. Cimen, and Q. M. Zhu, *Decentralised Load Frequency Controller Design based on Structured Singular Values*, *IEE Proceedings on Generation, Transmission and Distribution*, Vol. 145, No. 1, 1998, pp. 7–14.
- [31] M. S. Yousuf, H. N. Al-Duwaish, and Z. M. Al-Hamouz, *PSO Based Predictive Nonlinear Automatic Generation Control*, *WSEAS Automatic Control, Modelling and Simulation Conference*, 2010, pp. 87–92.

- [32] M. Zribi, M. Al-Rashed, and M. Alrifai, *Adaptive Decentralized Load Frequency Control of Multi-area Power Systems*, *Electrical Power and Energy Systems*, Vol. 27, 2005, pp. 575-583.